
EDDY COVARIANCE TOWERS AS SENTINELS OF ABNORMAL RADIOACTIVE MATERIAL RELEASES

THIS IS A DRAFT OF A MANUSCRIPT INTENDED FOR ENVIRONMENTAL SCIENCE AND POLLUTION RESEARCH
DOI: 10.1000/XXXXX

 **Corresponding Author: Jemma Stachelek¹**

¹ High Performance Computing Division
Los Alamos National Laboratory
Los Alamos, NM, USA, 87544
jsta@lanl.gov

Vachel A. Kraklow²

² Earth and Environmental Sciences Division
Los Alamos National Laboratory
Los Alamos, NM, USA, 87544

Elizabeth Christi Thompson³

³ Computer, Computational, and Statistical Sciences Division
Los Alamos National Laboratory
Los Alamos, NM, USA, 87544

Lee Turin Dickman²

² Earth and Environmental Sciences Division
Los Alamos National Laboratory
Los Alamos, NM, USA, 87544

Emily Casleton³

³ Computer, Computational, and Statistical Sciences Division
Los Alamos National Laboratory
Los Alamos, NM, USA, 87544

Sanna Sevanto²

² Earth and Environmental Sciences Division
Los Alamos National Laboratory
Los Alamos, NM, USA, 87544

Ann Junghans⁴

⁴ Nuclear and Engineering Nonproliferation Division
Los Alamos National Laboratory
Los Alamos, NM, USA, 87544

1 Abstract

2 Ensuring accurate detection and attribution of abnormal releases of radioactive material is critical for protecting human
3 health and safety. Most commonly, such detection is accomplished via active monitoring approaches involving the
4 collection of physical samples. This is labor intensive and limits the temporal and spatial resolution of any detected
5 events to a relatively coarse level. As an alternative first step towards passive monitoring, we developed an approach
6 using eddy flux tower data records to identify signals from a known abnormal release and quantify the extent to which
7 that signal also occurs at other times in the data record. Through two case-studies, one of which targeted the Fukushima
8 nuclear disaster and the other targeting an abnormal release event at a radioisotope production facility in Fleurus
9 Belgium, we tested our approach and identified several potential heretofore unidentified abnormal events that were
10 consistent with atmospheric circulation patterns and/or wind direction from known release sites. Because our approach
11 is relatively simple and is resistant to systematic errors in the observational record, it has broad applicability beyond
12 specific constituents and ecosystem types to identify a wide variety of limited-duration anomalies in flux tower data to
13 ensure human health and industrial safety.

14 **Keywords:** eddy covariance, data mining, industrial safety, vegetation response, radioactivity, photosynthesis

15 1 Introduction

16 Detecting abnormal releases of radioactive material (hereafter simply “abnormal releases”) is important as a means
17 of ensuring human health and industrial safety. The detection of such releases is typically accomplished using active
18 approaches that require site-specific sampling or trace gas measurements (Loyalka, 1983) sometimes as a part of
19 international monitoring networks (e.g., Sangiorgi et al., 2020). A potential shortcoming of these active monitoring
20 approaches is that they require collection of physical samples (particulates, gasses, and other signal carriers) to
21 retrospectively determine the nature of the release and the events that may have led up to it. Active monitoring with
22 such means is thus labor intensive and limits the temporal and spatial resolution of any detected events to a relatively
23 coarse level.

24 A potential alternative to active monitoring is passive monitoring (e.g., the German Integrated Measuring and Information
25 system and the International Monitoring System, Bieringer and Schlosser, 2004). Although existing wide area
26 monitoring systems are already critical components of abnormal release detection and tracking programs (Medici, 2001),
27 diversification-of-approach may increase the programs’ sensitivity and comprehensiveness. With a greater diversity
28 of methods, monitoring programs may be able to detect a wider array of constituents with differing characteristics or
29 expand their geographic extent without the need to deploy new instrumentation. In the present study, we developed a
30 novel passive monitoring approach to supplement existing programs that involves the use of eddy covariance data to
31 capture a signal from known abnormal releases. This signal is then used to investigate whether additional potential
32 abnormal releases exist at other times in the data record. We focused on eddy flux towers, as they have the potential
33 to provide abnormal release signatures, are globally distributed, have been in near continuous operation for several
34 decades, and can be relatively cheaply and easily deployed in locations of interest. Therefore, they constitute a rich
35 target for data mining approaches aimed at identifying signatures resulting from direct interference of radioactive
36 material with target measurements and/or the indirect signal of vegetation responses to the deposition of radioactive
37 material.

38 Our utilization of flux tower records for event discrimination stands in contrast to the typical use of data from the
39 towers for direct carbon balance accounting. Whereas carbon balance accounting activities deal directly in the units of
40 the measured data for computing quantities like net ecosystem exchange (Baldocchi et al., 2018), our use treats each
41 variable as potentially including an indirect signal (i.e. an anomaly from normal vegetation behavior) of radioactive
42 material deposition irrespective of its physical properties (e.g., mass, volume, etc). In this way, we are not directly
43 measuring radioactive deposition but rather leveraging the fact that existing ecosystem monitoring records reflect
44 vegetation photosynthesis rates and general stress condition of site vegetation in a known way (Nobel, 2020).

45 We specifically focused on short-term anomalies in the vegetation response data (on the order of days to weeks) due
46 to either potential deposition of radioactive material or direct sensor effects rather than chronic long-term signals
47 on the order of years to decades. In the first case study, we tested the ability of various data mining techniques to
48 recover the signal from the closest tower (approximately 18 km away) to a known release coming from the Institut

des Radioelements (IRE) in Belgium nominally occurring on August 23, 2008. This release originated from waste tanks into the atmosphere and lasted for several days totaling 50 GBq ^{131}I . The release went unreported (and possibly undetected) for several days. The first measurements in the vicinity of the facility were not taken until August 28th. These measurements found radioactivity levels of 5,000 Bq/kg in grass samples and led to a public health advisory for a 5km zone extending in a northeasterly direction from the facility (Carlé et al., 2010). Owing to the aforementioned measurement delays and the limited extent of the IRE release, we lack numeric estimates of the activity concentrations at tower locations. In the second case study, we further explored potential signals in flux tower data related to the Fukushima Nuclear Disaster occurring on March 11, 2011 releasing a massive radioactive plume that reached North America in 5 days that eventually dispersed throughout the entire northern hemisphere. An atmospheric dispersion study by Mészáros et al. (2016) estimates that our selected tower locations experienced deposition of particulate matter in the range of 0.44 - 31.08 mBq/m³.

We used the signal identified during the known release to identify additional potential abnormal releases occurring at other times in the data record and at other eddy flux towers. While the body of literature on direct or indirect effects of radioactive material on vegetation is limited, prior studies support the idea that exposure may cause declines in photosynthetic CO_2 uptake. For example, Gudkov et al. (2019) detail how a wide range of exposure doses and durations can inhibit CO₂ uptake as a result of enzymatic effects on the Calvin Cycle. For the present study, we lack leaf-level observations to directly establish inhibition and instead express it as a change in the slope of the CO_2 relationship with other environmental variables (e.g. air temperature, humidity, precipitation, etc.) before, during, and after exposure.

2 Methods

2.1 Data Description

For both the IRE and Fukushima case studiesy, we gathered measurements from eddy covariance platforms (i.e., “flux towers”) spanning multiple years. For the IRE case study, we targeted towers located in Belgium, which are part of the ICOS (Integrated Carbon Observation System) network available through the European Fluxes Database (<http://www.europe-fluxdata.eu/>). Three sites in proximity to the known release location had sufficient long-term data for our anticipated data mining efforts (BE-Lon, BE-Bra, and BE-Vie sites, Figure 1A). Each of the three flux tower sites are located within a crop ecosystem type and had almost 10 years of data available from 2004 through 2013 recorded at 30 min intervals. While BE-Lon had a near-continuous data record during this period, BE-Bra had a long period of missing data in 2005, and both BE-Bra and BE-Vie had a long period of missing data in 2009. The distance between IRE and the flux tower sites are approximately 19 km, 95 km, and 105 km for the BE-Lon, BE-Bra, and BE-Vie, respectively.

For the Fukushima case study, due to the direction of the plume, we gathered measurements from flux towers located in the Northern Hemisphere (Western United States), which are part of the Ameriflux network (<https://ameriflux.lbl.gov/>). To increase confidence that we are seeing a real effect, we contrasted the results from Northern Hemisphere sites, where

82 we expect a higher likelihood of impact, to measurements from flux towers located in the Southern Hemisphere, which
83 are part of the OzFlux network (Cleverly, 2011). We selected sites with sufficient long-term data to cover the 2011 date
84 of the disaster and excluded boreal sites with extreme snow cover related seasonality. We ultimately selected three sites
85 (US-Wrc, US-GLE, and OZ-Mul, Figure 1B).

86 **2.2 Statistical Approach**

87 We processed each data file by 1) excluding nighttime measurements based on photosynthetic photon flux density
88 (PPFD > 100 $\mu\text{mol m}^{-2} \text{s}^{-1}$) or net solar radiation (netrad > 0 W/m^2) and 2) defining an “event period” following
89 the publicly released date of the abnormal release. We focused on the following variables as potentially containing a
90 signature of the release : carbon dioxide, carbon dioxide flux (fc), latent heat (le), and sensible heat flux (h). Conversely,
91 the following were treated as independent explanatory variables: wind speed, precipitation, atmospheric pressure,
92 relative humidity, photosynthetic photon flux density, air temperature, and net radiation. Additionally, we used wind
93 direction data from the eddy flux towers to determine when or if any released material might plausibly reach a particular
94 location. All of the aforementioned data for each of these variables obtained from flux tower instrumentation recorded
95 at a 30 minute (min) interval barring any gaps due to missing data.

96 To begin our analysis, we screened all pairwise, linear relationships between the aforementioned independent and
97 dependent variables using a linear regression fit between each pair for the entire period of record (n=51). Variable
98 pairs were excluded from further analysis if the overall coefficient of determination (R^2) was less than 0.1. This low
99 threshold was chosen to maximize the number of pairs that could potentially be investigated more deeply. From visual
100 inspection, we determined that many of the rejected variable pairs appeared to have a nonlinear relationship. As our
101 aim was to develop a methodology that could be applied broadly to other sites, we did not apply transformation to
102 linearize these relationships without a physical justification for the transformation. Evaluating an exhaustive list of data
103 transformations was beyond the scope of the present effort. After identification of candidate variable pairs, we fit an
104 interaction model of the following form where Y represents a continuous response (e.g., CO_2 , latent heat, etc.), X_1 is
105 an independent variable (e.g., air temperature, humidity, etc.), W_2 is a categorical variable representing the “period”
106 of observation (i.e., during, before, or after, the event), β_0 is the intercept, $\beta_{1,2}$ are slope parameters for X_1 and W_2
107 respectively, and β_3 is the slope parameter for the interaction between X_1 and W_2 :

$$Y = \beta_0 + \beta_1 X_1 + \beta_2 W_2 + \beta_3 X_1 W_2$$

108 This interaction model was fit for a window of time encompassing the known release event and for every other possible
109 window in the period-of-record. The overall length of the window was treated as an adjustable hyperparameter since
110 the length of time for an abnormal material release to reach the footprint of the flux tower may be event-dependent
111 and/or unknown. In addition, the length of time for deposited material to induce a possible vegetation response (or at
112 least a flux data anomaly) is an unknown quantity. Thus, in the default base case, we set the window length (n_days)

as 7 days, but we ran hyperparameter experiments to determine the result of setting it to longer periods of 10 and 14 days. The window length affects the duration of time designated as before and after the event. The period of time designated as during the event was set as 2 days in all cases. We compared the effect size of the interaction term (β_3) during the event-encompassing window against all other windows in a “rolling” analysis. Therefore, the overall analysis compares the interaction term of the window of the known event against a window centered on every other observation. Specific windows that had an effect size at least as large as that of the known event and with wind conditions defined as “towards” the flux tower were flagged as “event detections”.

In order to flag event detections, we defined several adjustable hyperparameters to account for uncertainty surrounding atmospheric transport and the timing of any possible responses to material deposition. The first hyperparameter we defined, `wind_tolerance`, reflects the range around the bearing from the facility to the tower location which counts as towards the tower. In the base default case, we set `wind_tolerance` to 10 degrees, but we explored setting it to smaller values down to 5 degrees and larger values up to 20 degrees. The second hyperparameter we defined, `event_quantile_effect`, handles the unknown travel time of any materials to be deposited via an abnormal release or what, if any, delays exist between deposition and vegetation response. Rather than simply selecting the maximum value of β_3 during a given window or the value at the exact time of the event, the value of `event_quantile_effect` is set to correspond with a specific quantile of all β_3 values during the event window. In the base default case, this was set at 0.9, but we explored values as low as 0.5. All statistical analyses were carried out using the `statsmodels` Python package (Seabold and Perktold, 2009). Our processing scripts are openly available at [doi link], and we refer readers to the original providers for data access.

3 Results

For the IRE case study, among all possible pairwise combinations of dependent and independent variables (n=51, Table S1), we found that only the CO_2 versus air temperature comparison had any measure of predictability from the model ($R^2 > 0.05$) and a strong event effect size (Table 1). Although other variable pairs such as sensible heat flux and net radiation had a stronger effect size for the BE-Lon site, they had a weak linear relationship across the other sites. When we focus on the period of the abnormal release event in particular rather than the overall period of record, we found that CO_2 versus air temperature relationship at each of the three focal towers had similar R^2 values and effect sizes (Table 1). Figure 2 provides a visual example of the effect size framing in our analysis. Note how the apparent interaction effect between time periods around the abnormal release event in Figure 2A (before, during, after) translates to a relatively high effect size (Figure 2C) whereas in Figure 2B at an arbitrary time point, there is no apparent interaction effect. This corresponds to a low effect size in Figure 2D. Note also how during and after the known abnormal release, the slopes of the relationships between CO_2 and air temperature become less negative than before the event, with lower than expected CO_2 at low air temperature (Figure 2A).

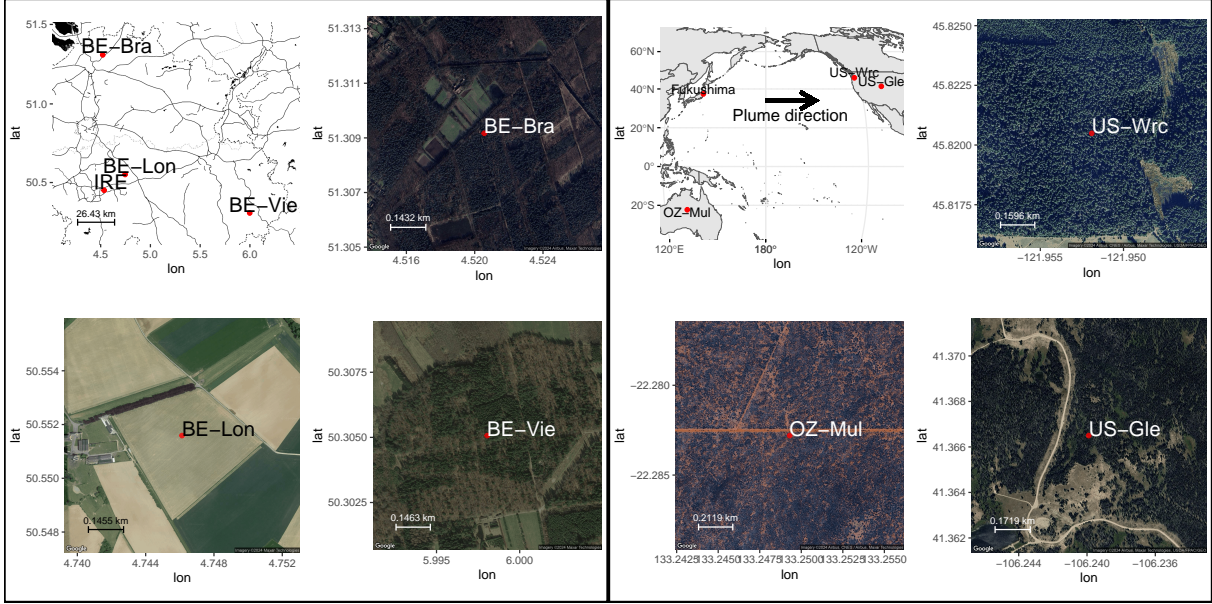


Figure 1: Map of flux tower locations for the IRE and Fukushima case studies (left and right respectively). Note that BE-Lon and BE-Vie are of a similar easterly direction to the IRE site whereas BE-Bra is in a northerly direction. The distance between IRE and the flux tower sites are approximately 19, 95, and 105 km for the BE-Lon, BE-Bra, and BE-Vie respectively. Each of the three IRE flux tower sites are located within a crop ecosystem type. Note that the US-Wrc site would be expected to have first contact with the Fukushima atmospheric plume followed by US-Gle. The OZ-Mul site would not be expected to have been affected by the plume.

145 Despite the similar effect size at the three tower sites during the abnormal release event, they differed substantially in
 146 the degree to which they uniquely flagged the known release event. At the BE-Lon and BE-Vie sites, our event detection
 147 algorithm identified the known release and only a few other time periods as potential abnormal releases (Figure 3).
 148 Conversely, at the northerly BE-Bra site, the algorithm was not able to identify the known release event distinct from
 149 background noise. This can be seen in the rate of event detections (α) at each site, whereby it was less than 1% at the
 150 BE-Lon and BE-Vie sites, but was greater than 2% at the BE-Bra site. It is notable that this ability to uniquely detect
 151 the known release along with a plausible number of additional event detections corresponds with the fraction of the
 152 abnormal release period when the wind was pointed from the release location towards the respective tower (using the
 153 default base case wind tolerance of 10 deg) which was much lower at the BE-Bra site (5%) compared to the BE-Lon
 154 and BE-Vie sites (34% Table 1).

155 To increase our confidence that event detections were not dependent on the specific hyperparameters settings in our
 156 base-case setup, we ran an exhaustive cross-validation set of hyperparameter experiments. For this effort, we tested
 157 every possible combination of values for wind tolerance, number of days, and the event quantile effect. Across
 158 reasonable values of specific hyperparameters, we found that their magnitudes had little effect on the rate at which
 159 events were flagged as potential abnormal releases as even in the most extreme cases, we did not see detection rates
 160 exceeding 1%. We did, however, observe that the event detection was related to the window length and event quantile
 161 parameters as shown by the slope of the line in Figure 4. Although increasing values of the event quantile parameter
 162 would hypothetically increase event detection rates, we do not see value in setting this parameter below the median.

Table 1: Overview of CO_2 vs air temperature interaction models at the IRE site. R^2 is the coefficient of determination of a linear model fit to the two covariates for the period of the abnormal release event (corresponding to “during” in Fig. 2). Effect is the event effect size of the interaction term ‘during’ the known release period matching the quantile of the distribution as specified by event quantile effect hyperparameter. Wind (%) is the average percentage of time that wind direction was from the site of known release towards the selected flux tower during the known release event. The remaining columns indicate the base-case hyperparameter settings.

Site	R^2	Effect	Wind(%)	Days(n)	Wind(tol)	Effect(q)
BE-Vie	0.35	36.2	34	7	10	0.9
BE-Bra	0.4	57.59	5	7	10	0.9
BE-Lon	0.47	30.13	34	7	10	0.9

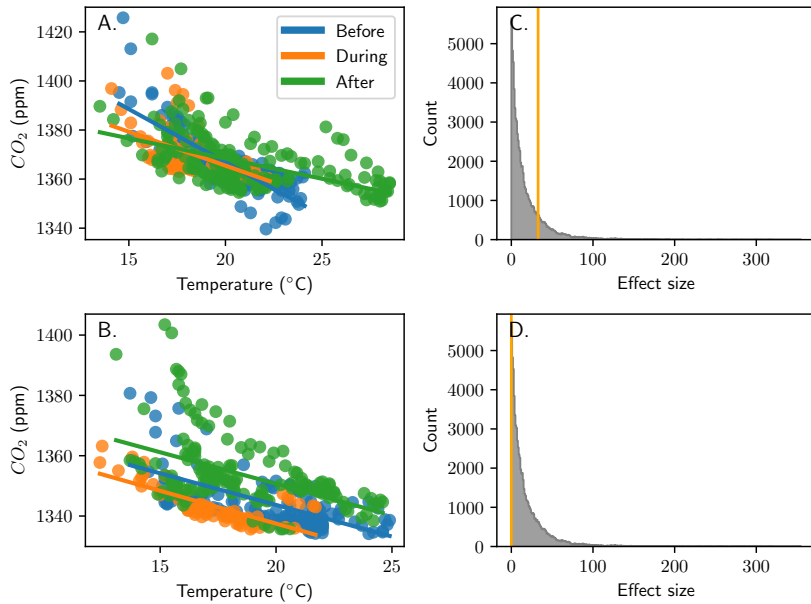


Figure 2: Interaction plots at the BE-Lon site between air temperature (C°) and CO_2 (ppm) for the period of the known abnormal release (A) and an arbitrary non-release period (B). Also shown is the distribution of all interaction effect sizes (gray) compared with the effect size of the time period shown in the corresponding left panels (orange, C, D).

- 163 Similarly, increasing the magnitude of the window length parameter would also likely increase the event detection
 164 rate but here too we do not see value in setting this parameter beyond 14 days given the results of prior atmospheric
 165 modeling efforts (e.g. Mészáros et al., 2016).
- 166 For the Fukushima case study, our objective was to test the sensitivity of our approach to a broad scale abnormal release
 167 and to introduce a control design to verify behavior on a flux tower where we expect no impact from any abnormal
 168 releases. First, we verified that event detection specificity is present at towers likely to be exposed even across long
 169 distances if the abnormal release is large (Figure 5). Then, we found a decrease in event detection specificity and an
 170 increase in event detection rate moving from the flux tower expected to be most affected (US-Wrc), to a more distant
 171 (likely less affected) tower (US-Gle), to a tower likely not exposed at all to the atmospheric plume (OZ-Mul, Figure 5).

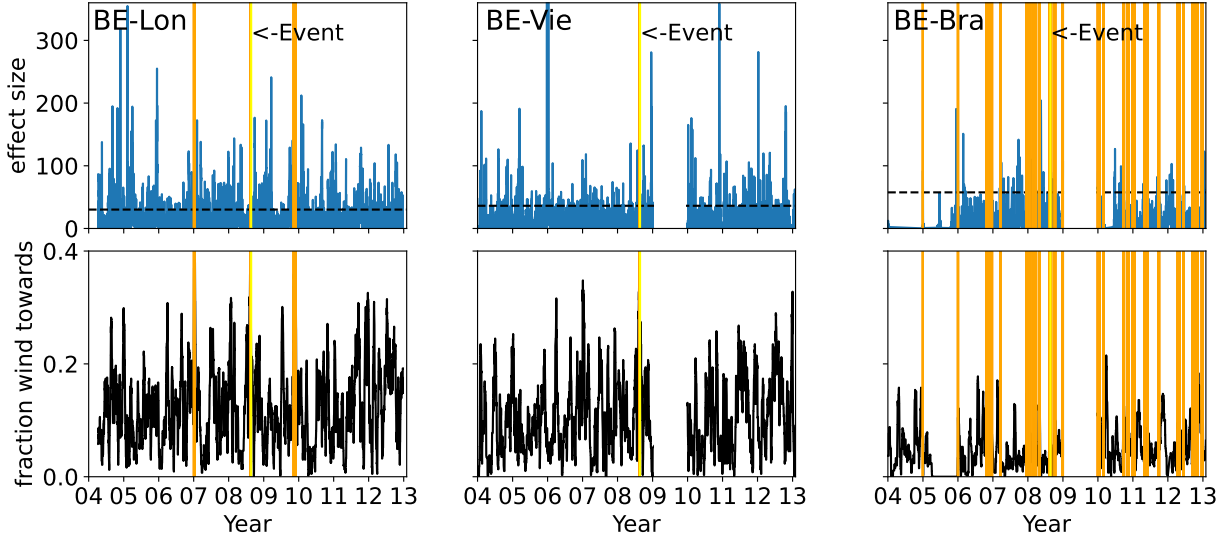


Figure 3: Time series plots (2004-2013) of rolling event detection analysis at the IRE site for the CO_2 and air temperature (C°) variable pair. Event detection lines (orange), interaction effect size (blue), and event effect size (dashed black line) are shown in the top panels. The fraction of time that the wind direction was towards the particular tower (solid black) are shown in the corresponding bottom panels.

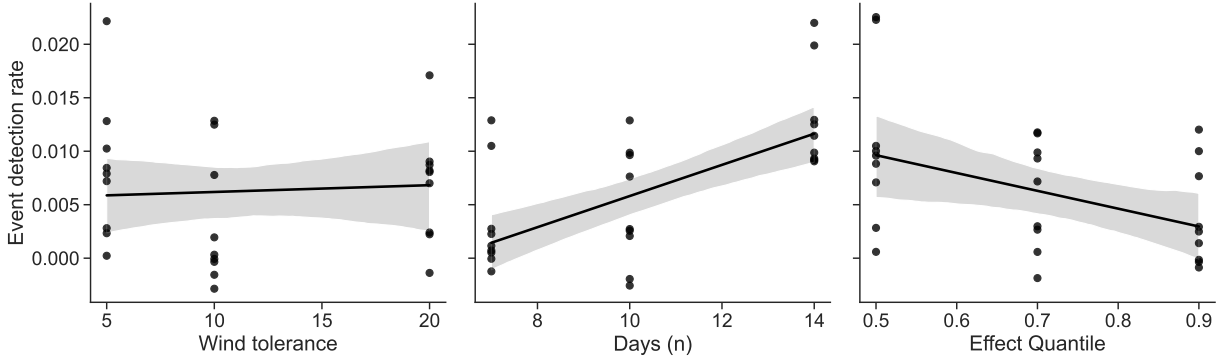


Figure 4: Sensitivity of event detection at the IRE site to different hyperparameter values (points) alongside potential relationship (solid line) and confidence interval (shaded region).

172 4 Discussion

173 Using flux tower records collected closest to and in the prevailing wind direction to the IRE and the Fukushima release
 174 locations, our event detection algorithm was able to identify both known abnormal releases and plausible previously
 175 unidentified abnormal events. There was broad agreement among the closest flux tower and more distant flux towers
 176 as to the timing and frequency of these releases, and our approach was supported by the loss of signal at flux towers
 177 outside of the prevailing wind direction. This suggests that, at the very least, given a facility known to have a prior
 178 abnormal release, flux tower networks are capable of providing a means of passive monitoring to detect subsequent
 179 events as well as information on the environmental conditions before, during, and after the event. Furthermore, our
 180 approach has promise for situations when there is not a prior known abnormal release. In these cases, it may be possible
 181 to continuously mine flux tower records (as they become available) for events that exceed some threshold identified in a

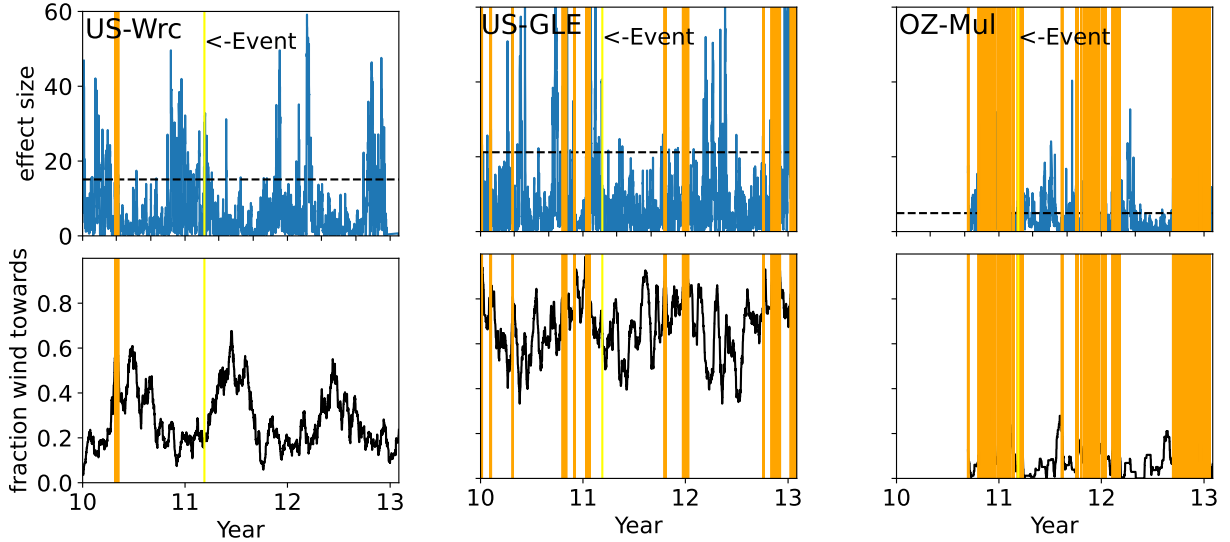


Figure 5: Time series plots (2010-2013) of rolling event detection analysis for the Fukushima disaster case study. The depicted variable pair is latent heat and relative humidity. Event detection lines (orange), interaction effect size (blue), and event effect size (dashed black line) are shown in the top panels. The fraction of time that the wind direction was towards the particular tower (solid black) are shown in the corresponding bottom panels.

more comprehensive cross-site, cross-event benchmarking study. The delay between data collection and availability to the general community is highly variable among sites and investigators. In the best case scenario, for actively monitored sites with responsive investigators, this can be as little as 6 months. As a result, operationalization of our approach might target post-hoc attribution rather than real-time monitoring applications.

More generally, we show that flux tower records have value for this type of data mining despite the apparent noisiness of the data (e.g., Fratini et al., 2018). We attribute the sensitivity of our approach to the fact that we fit successive interaction models to limited sections of the data record, and we leveraged bivariate relationships to constrain noisiness in individual data records. Our approach was aided by the fact that this type of scale-free data mining is largely unaffected by systematic errors due to uncertainty in calibration standards and/or low resolution in specific sensor packages deployed on the towers. This is because although such systematic errors may bias the magnitude of overall flux values, which would be a problem for typical uses of flux towers that deal directly in the units of the measured data, they do not reduce the overall confidence in individual values (Langford et al., 2015), which for our purposes might represent an abnormal release signal. The ability of our approach to identify a suitable release signature does likely depend on the quality and completeness of the underlying data.

Another contributor to the success of our approach was our ability to compare event detections at close towers in prevailing wind directions against more distant towers (refer to Figure 1), increasing our confidence that we were seeing a true signal and not spurious noise. The relatively dense networks of flux towers with long data records leveraged in both locations also aided these case studies. This level of flux tower density may be found in the United States, Western/Central Europe, Japan, and Australia, which have high densities of flux towers, but not throughout the rest of the world (Baldocchi et al., 2001; Pastorello et al., 2020). As a result, this may impose geographical limits on

202 our approach, although installation and maintenance of new flux towers in locations of interest may be cost effective
203 compared to other monitoring approaches. Another attribute that likely aided our investigations was the fact that all
204 three of the flux towers we examined were located in similar agricultural and forested ecosystem types for the IRE and
205 Fukushima case studies respectively. Although investigating whether or not flux tower combinations with differing
206 ecosystems would yield similar results is beyond the scope of the present study, we suspect that the data records among
207 towers in disparate ecosystem types could differ too drastically to be of comparative use. For example, Pastorello et al.
208 (2020) show that towers in the crop ecosystem type, of which all three sites used in this study belong, have a relatively
209 narrow distribution of fluxes (i.e., gross primary production, GPP) compared to towers in the grassland or evergreen
210 broadleaf forest types. One reason for this narrow spread in crop ecosystems may be the relative homogeneity of flux
211 tower footprints in crop ecosystems, which typically extend to within 1000m of the tower depending on atmospheric
212 conditions (e.g., wind speed and direction, Chu et al., 2021). Given that towers in other ecosystem types with a more
213 heterogeneous flux tower footprint have a wider distribution of fluxes (e.g. Pastorello et al., 2020), we suspect that
214 having all the towers in the IRE case study located in a homogenous ecosystem type was helpful in reducing the
215 spikiness and spread of the data.

216 The biggest improvements to our approach would likely come from coupling our data mining procedure with rigorous
217 air pollutant dispersion modeling (e.g., Mészáros et al., 2016). This would eliminate the need for indirect estimation
218 of material transport via uncertainty analyses and instead use simulation results to analytically determine the likely
219 arrival and duration of material deposition. Further improvements could be made by incorporating knowledge about
220 the composition of materials being deposited (IAEA, 2006; Mészáros et al., 2016) and/or the interactions between
221 material exposure and other environmental stressors (Mousseau and Møller, 2020), which likely affects the severity
222 and timing of ecosystem responses and by extension the fluxes being measured by a given tower. Such information
223 may help disentangle potential interference of atmospheric contaminants with infrared measurement of CO_2 from
224 declines in photosynthetic CO_2 uptake of contaminated vegetation given our observation that during and after the
225 known abnormal release, the slopes of the relationships between CO_2 and air temperature become less negative than
226 before the event, with lower than expected CO_2 at low air temperature. Although the chemical makeup of possible
227 atmospheric contaminants is unknown, interference by iodine itself is unlikely to affect measurements of CO_2 given
228 that the absorption spectra of iodine peaks at much shorter wavelengths around 10-7 m (Haynes, 2016) compared to
229 that of CO_2 which peaks around 1700-2100 10-9 m (LICOR Biosciences Inc., Lincoln, NE).

230 The fact that we were able to identify known releases (along with potential unidentified abnormal events) in the data
231 records from both a large event (i.e. Fukushima) as well as a smaller event despite not having a detailed radiological or
232 atmospheric transport model is a strength of our approach. Furthermore, our approach is not limited to a radiological
233 context, any abnormal event that affects the plant community and is reflected in flux tower data is a potential target.
234 Because our approach is light-weight and resistant to systematic errors in the observational record, it has broad
235 applicability beyond specific constituents and ecosystem types to identify a wide variety of limited-duration impacts to
236 the plant community within flux tower footprints to ensure human health and industrial safety.

237 References

- 238 Baldocchi, D., Falge, E., Gu, L., Olson, R., Hollinger, D., Running, S., Anthoni, P., Bernhofer, C., Davis, K., Evans, R.,
239 et al., 2001. FLUXNET: A new tool to study the temporal and spatial variability of ecosystem-scale carbon dioxide,
240 water vapor, and energy flux densities. *Bulletin of the American Meteorological Society*, 82(11):2415–2434.
- 241 Baldocchi, D., Chu, H., and Reichstein, M., 2018. Inter-annual variability of net and gross ecosystem carbon fluxes: A
242 review. *Agricultural and Forest Meteorology*, 249:520–533. doi:10.1016/j.agrformet.2017.05.015.
- 243 Bieringer, J. and Schlosser, C., 2004. Monitoring ground-level air for trace analysis: Methods and results. *Analytical
244 and Bioanalytical Chemistry*, 379(2):234–241. doi:10.1007/s00216-004-2499-z.
- 245 Carlé, B., Perko, T., Turcanu, C., and Schröder, J., 2010. Individual response to communication about the August 2008
246 131I release in Fleurus: Results from a large scale survey with the Belgian population. *Session 19: Radiation and the
247 society*, page 2774.
- 248 Chu, H., Luo, X., Ouyang, Z., Chan, W. S., Dengel, S., Biraud, S. C., Torn, M. S., Metzger, S., Kumar, J., Arain,
249 M. A., Arkebauer, T. J., Baldocchi, D., Bernacchi, C., Billesbach, D., Black, T. A., Blanken, P. D., Bohrer, G.,
250 Bracho, R., Brown, S., Brunsell, N. A., Chen, J., Chen, X., Clark, K., Desai, A. R., Duman, T., Durden, D., Fares, S.,
251 Forbrich, I., Gamon, J. A., Gough, C. M., Griffis, T., Helbig, M., Hollinger, D., Humphreys, E., Ikawa, H., Iwata,
252 H., Ju, Y., Knowles, J. F., Knox, S. H., Kobayashi, H., Kolb, T., Law, B., Lee, X., Litvak, M., Liu, H., Munger,
253 J. W., Noormets, A., Novick, K., Oberbauer, S. F., Oechel, W., Oikawa, P., Papuga, S. A., Pendall, E., Prajapati,
254 P., Prueger, J., Quinton, W. L., Richardson, A. D., Russell, E. S., Scott, R. L., Starr, G., Staebler, R., Stoy, P. C.,
255 Stuart-Haëntjens, E., Sonnentag, O., Sullivan, R. C., Suyker, A., Ueyama, M., Vargas, R., Wood, J. D., and Zona, D.,
256 2021. Representativeness of Eddy-Covariance flux footprints for areas surrounding AmeriFlux sites. *Agricultural
257 and Forest Meteorology*, 301–302:108350. doi:10.1016/j.agrformet.2021.108350.
- 258 Cleverly, J., 2011. Alice springs mulga OzFlux site. *OzFlux: Australian and New Zealand flux research and monitoring
259 network, hdl*, 102(100):8697.
- 260 Fratini, G., Sabbatini, S., Ediger, K., Riensche, B., Burba, G., Nicolini, G., Vitale, D., and Papale, D., 2018. Eddy
261 covariance flux errors due to random and systematic timing errors during data acquisition. *Biogeosciences*, 15(17):
262 5473–5487. doi:10.5194/bg-15-5473-2018.
- 263 Gudkov, S. V., Grinberg, M. A., Sukhov, V., and Vodeneev, V., 2019. Effect of ionizing radiation on physiological and
264 molecular processes in plants. *Journal of Environmental Radioactivity*, 202:8–24. doi:10.1016/j.jenvrad.2019.02.001.
- 265 Haynes, W. M., 2016. *CRC Handbook of Chemistry and Physics*. CRC press.
- 266 IAEA, 2006. *Radiological Conditions in the Dnieper River Basin*. Radiological Assessment Reports Series. International
267 Atomic Energy Agency, Vienna. ISBN 92-0-104905-6.

- 268 Langford, B., Acton, W., Ammann, C., Valach, A., and Nemitz, E., 2015. Eddy-covariance data with low signal-to-noise
269 ratio: Time-lag determination, uncertainties and limit of detection. *Atmospheric Measurement Techniques*, 8(10):
270 4197–4213. doi:10.5194/amt-8-4197-2015.
- 271 Loyalka, S., 1983. Mechanics of aerosols in nuclear reactor safety: A review. *Progress in Nuclear Energy*, 12(1):1–56.
272 doi:10.1016/0149-1970(83)90024-0.
- 273 Medici, F., 2001. The IMS radionuclide network of the CTBT. *Radiation Physics and Chemistry*, 61(3-6):689–690.
274 doi:10.1016/S0969-806X(01)00375-9.
- 275 Mészáros, R., Leelőssy, Á., Kovács, T., and Lagzi, I., 2016. Predictability of the dispersion of Fukushima-derived
276 radionuclides and their homogenization in the atmosphere. *Scientific Reports*, 6(1):19915. doi:10.1038/srep19915.
- 277 Mousseau, T. A. and Møller, A. P., 2020. Plants in the Light of Ionizing Radiation: What Have We Learned From
278 Chernobyl, Fukushima, and Other “Hot” Places? *Frontiers in Plant Science*, 11:552. doi:10.3389/fpls.2020.00552.
- 279 Nobel, P., 2020. *Physicochemical and Environmental Plant Physiology*. Elsevier. ISBN 978-0-12-819146-0.
280 doi:10.1016/C2018-0-04662-9.
- 281 Pastorello, G., Trotta, C., Canfora, E., Chu, H., Christianson, D., Cheah, Y.-W., Poindexter, C., Chen, J., Elbashandy, A.,
282 Humphrey, M., et al., 2020. The FLUXNET2015 dataset and the ONEFlux processing pipeline for eddy covariance
283 data. *Scientific data*, 7(1):225.
- 284 Sangiorgi, M., Hernández-Ceballos, M. A., Jackson, K., Cinelli, G., Bogucarskis, K., De Felice, L., Patrascu, A., and
285 De Cort, M., 2020. The European Radiological Data Exchange Platform (EURDEP): 25 years of monitoring data
286 exchange. *Earth System Science Data*, 12(1):109–118. doi:10.5194/essd-12-109-2020.

287 **Statements and Declarations**

288 **Funding**

289 We acknowledge funding for supporting the AmeriFlux data portal: U.S. Department of Energy Office of Science.
290 The data used in this activity has been also funded by CarboEuropeIP (EU-FP6), IMECC (EU-FP6). This work was
291 supported by Los Alamos National Laboratory (LDRD-20220062ER).

292 **Competing Interests**

293 The authors have no relevant financial or non-financial interests to disclose.

294 **Author Contributions**

295 JS built models, analyzed data, and wrote the paper. SS, LTD, and AJ contributed to the conception of the manuscript.
296 ECT, VAK, LTD, and EC edited the manuscript. All authors provided interpretation of results.

297 Ethical Approval

298 Not applicable

299 Consent to Participate

300 Not applicable

301 Consent to Publish

302 Not applicable

303 Availability of Data and Materials

304 No new data was produced in this study. All original data used is available publicly from their respective sources and
305 archived permanently with restrictions on redistribution. These can be found at <http://www.europe-fluxdata.eu/>,
306 <https://fluxnet.org/>, and (Cleverly, 2011).

307 Computer code and secondary data reuse that supports the results and analyses of the paper are available at:
308 <https://doi.org/10.5281/zenodo.13845254>.